Weierstraß-Institut
für Angewandte Analysis und Stochastik
Leibniz-Institut im Forschungsverbund Berlin e. V.

Preprint ISSN 2198-5855

Turbulence in the Ott-Antonsen equation for arrays of coupled phase oscillators

Matthias Wolfrum[1], Svetlana V. Gurevich[2], Oleh E. Omel'chenko[1]

submitted: June 24, 2015

[1] Weierstrass Institute
Mohrenstr. 39
10117 Berlin
Germany
E-Mail: Matthias.Wolfrum@wias-berlin.de
Oleh.Omelchenko@wias-berlin.de

[2] Institute for Theoretical Physics
University of Münster
Wilhelm-Klemm-Str. 9
48149 Münster
Germany
E-Mail: gurevics@uni-muenster.de

No. 2135
Berlin 2015

2010 *Mathematics Subject Classification.* 34C15, 37N20, 37N25.

2008 *Physics and Astronomy Classification Scheme.* 05.45.Xt, 89.75.Kd.

Key words and phrases. Coupled oscillators, Kuramoto model, twisted states, turbulence, Ott/Antonsen, Eckhaus scenario.

M. W. gratefully acknowledges support by The Einstein Center for Mathematics Berlin (Project D-OT2), and O. O. by the Collaborative Research Center 910.

Edited by
Weierstraß-Institut für Angewandte Analysis und Stochastik (WIAS)
Leibniz-Institut im Forschungsverbund Berlin e. V.
Mohrenstraße 39
10117 Berlin
Germany

Fax: +49 30 20372-303
E-Mail: preprint@wias-berlin.de
World Wide Web: http://www.wias-berlin.de/

Abstract

In this paper we study the transition to synchrony in an one-dimensional array of oscillators with non-local coupling. For its description in the continuum limit of a large number of phase oscillators, we use a corresponding Ott-Antonsen equation, which is an integro-differential equation for the evolution of the macroscopic profiles of the local mean field. Recently, it has been reported that in the spatially extended case at the synchronization threshold there appear partially coherent plane waves with different wave numbers, which are organized in the well-known Eckhaus scenario. In this paper, we show that for Kuramoto-Sakaguchi phase oscillators the phase lag parameter in the interaction function can induce a Benjamin-Feir type instability of the partially coherent plane waves. The emerging collective macroscopic chaos appears as an intermediate stage between complete incoherence and stable partially coherent plane waves. We give an analytic treatment of the Benjamin-Feir instability and its onset in a codimension-two bifurcation in the Ott-Antonsen equation as well as a numerical study of the transition from phase turbulence to amplitude turbulence inside the Benjamin-Feir unstable region.

According to the classical results of Yoshiki Kuramoto [13], increasing the coupling strength in a heterogeneous ensemble of globally coupled oscillators one can observe a transition from complete incoherence to partial synchrony at a certain critical coupling strength. Beyond this synchronization threshold there is a monotonic growth of the global order parameter, measuring the total amount of synchrony in the ensemble. For the description of more general interactions between the oscillators, Kuramoto and Sakaguchi introduced a phase-lag parameter in the sinusoidal interaction function, governing the attraction or repulsion between the oscillators. It has been shown that within the attractive regime the fundamental synchronization scenario is qualitatively not affected by this phase-lag parameter, at least for standard choices of the distribution of natural frequencies like Gaussian or Lorentzian. Only recently, it has been shown that for bimodal frequency distributions [19], certain unimodal distributions [22, 23], or more general phase interaction functions [12] one can expect various types of non-universal transitions to synchrony.

It was again Kuramoto in his work with Battogtokh [14], who pointed out that in spatially extended systems of coupled oscillators one can observe highly non-trivial states of self-organized coherence-incoherence patterns, now called *chimera states* [1], for which the phase lag parameter plays a crucial role. This newly discovered dynamical phenomenon has attracted a lot of research activities in the last decade (see [27] and references therein), including also various experimental realizations [32, 10, 20, 29, 11]. In this paper, we go back one step and study such systems of one-dimensional arrays of heterogeneous Kuramoto-Sakaguchi phase oscillators at the synchronization threshold where the completely incoherent state loses its stability and stable non-trivial solutions with collective motion and partial local synchrony appear. As we will show, the phase lag parameter plays in this case again a central role. In [33] it has been

shown that one-dimensional arrays of identical oscillators can give rise to spatially discretized plane wave solutions, which were called “twisted states”. In [24] it has been shown that for heterogeneous oscillators these solutions emerge successively after the synchronization threshold as partially coherent plane waves. They are organized in a Eckhaus scenario [9], where the partially coherent homogeneous solution, i.e. the wave with wave number zero, emerges stable as the primary central branch while the solutions with higher wave number bifurcate unstable at higher coupling from complete incoherence and gain their stability only for even higher coupling when they have reached a certain critical amplitude. We will now extend the analysis in [24] and study in more detail the stability properties of the partially coherent plane wave solutions. First, we derive explicit formulas for the Benjamin-Feir instability of partially coherent twisted states. Then, we show that due to the influence of the phase lag parameter there appears a codimension-2 bifurcations that changes the classical synchronization transition into a new scenario, where an intermediate state of collective macroscopic chaos appears between complete incoherence and stable partially coherent plane waves. We conclude with a numerical study of the Benjamin-Feir unstable region, where we determine the transition from phase turbulence to amplitude turbulence.

We are interested in one-dimensional arrays of non-identical phase-oscillators of the form

$$\frac{d\theta_k}{dt} = \omega_k - K\sum_j G_{kj}\sin(\theta_k - \theta_j + \alpha), \quad k = 1\ldots, N, \tag{1}$$

where the natural frequencies ω_k are drawn randomly and independently from the Lorentzian distribution

$$g_{\mathrm{L}}(\omega) = \frac{1}{\pi}\frac{1}{1+\omega^2}.$$

and the coupling coefficients G_{kj} are given by a non-negative piecewise-smooth kernel function $G(x)$

$$G_{kj} = \frac{1}{N}G\left(\frac{k-j}{N}\right),$$

which is even and non-increasing for $x \geq 0$, such that close oscillators in the array are coupled strongly, while more distant oscillators are coupled weaker. This system is typically equipped with periodic boundary conditions, i.e. considering the index of θ modulo N and assuming that $G(x) = 0$ for $|x| \geq \frac{1}{2}$, see e.g. [24].

Since we are interested in the collective motion in large systems of coupled oscillators, our starting point will be the formal continuum limit $N \to \infty$ [8, 31, 7]. In the case of purely sinusoidal coupling this limit can be written as an Ott-Antonsen equation of the form

$$\frac{du}{dt} = -u(x,t) + \frac{K}{2}e^{-i\alpha}\mathcal{G}u - \frac{K}{2}e^{i\alpha}u^2(x,t)\mathcal{G}\overline{u}. \tag{2}$$

An equation of this type has been introduced in [25, 26] for globally coupled systems. After that, generalizations of this approach to spatially extended systems [15] and several other more complicated settings have been presented [17, 18, 28, 16]. The basic idea of this approach is that complex-valued functions $u = u(x,t)$ that lie in the invariant set $|u| \leq 1$ and solve equation (2) can be identified with the macroscopic evolution of the local order parameter of

the oscillator system at a given position x and time t, such that the absolute value $|u(x,t)|$ measures the synchrony of oscillators with index close to $k = Nx$. and $\arg u(x,t)$ describes their most likely position on the unit circle.

The main parameters in equation (2) are the coupling strength $K > 0$ and the phase lag parameter α, which we restrict here to the attractive regime $\alpha \in (-\pi/2, \pi/2)$ where synchronization is possible. In the continuum limit, the non-local coupling between the oscillators is given by the convolution operator

$$(\mathcal{G}u)(x) = \int_{-\infty}^{\infty} G(x-y)u(y)dy \tag{3}$$

where we use again the function $G(x)$ with the properties as described above. Details of the derivation of a continuity equation for the probability densities describing the continuum limit and of the derivation of the Ott-Antonsen equation from this continuity equation can be found in [15, 24] where the same system has been investigated.

Note that referring to finite systems of oscillators with periodic boundary conditions this equation should be equipped with periodic boundary conditions as well. However, we are interested here in waves and spatial structures that are small compared to the total size of the domain and perform the analytical part of our investigations on the unbounded interval $x \in \mathbb{R}$.

Stability of the zero solution

We start with briefly recalling from [24] the results of a linear stability analysis of the zero solution. In order to deal with the complex-conjugated term $\overline{u}$, we will treat in the sequel the real and imaginary parts of Eq. (2) as a system of two real equations for the two unknown functions $\mathrm{Re}\, u$ and $\mathrm{Im}\, u$. This system defines a smooth dynamical system on the Banach space of uniformly bounded continuous functions $C(\mathbb{R};\mathbb{R}^2)$. Linearizing Eq. (2) around its zero solution we obtain

$$\frac{dv}{dt} = -v(x,t) + \frac{K}{2}e^{-i\alpha}\mathcal{G}v, \tag{4}$$

rewritten as a system in $\mathbb{R}^2$ as

$$\frac{dv_1}{dt} = -v_1 + \frac{K}{2}\left(\cos\alpha\ \mathcal{G}v_1 + \sin\alpha\ \mathcal{G}v_2\right), \tag{5}$$

$$\frac{dv_2}{dt} = -v_2 + \frac{K}{2}\left(-\sin\alpha\ \mathcal{G}v_1 + \cos\alpha\ \mathcal{G}v_2\right), \tag{6}$$

and look for its eigenfunctions in the following form

$$V = V_0 e^{i\kappa x} e^{\lambda t} \tag{7}$$

where $V_0 \in \mathbb{C}^2$, $\kappa \in \mathbb{R}$, and $\lambda \in \mathbb{C}$. Inserting ansatz (7) into Eqs. (5)–(6) and taking into account the identity

$$\int_{-\infty}^{\infty} G(x-y)e^{i\kappa y}dy = \hat{G}(\kappa)e^{i\kappa x}, \tag{8}$$

where

$$\hat{G}(\kappa) = \int_{-\infty}^{\infty} G(x)\cos(\kappa x)\,dx$$

is the Fourier transform of the coupling function $G(x)$, we obtain the characteristic equation

$$\chi_0(\lambda) = \det\begin{pmatrix} -1 + \frac{K}{2}\hat{G}(\kappa)\cos\alpha - \lambda & \frac{K}{2}\hat{G}(\kappa)\sin\alpha \\ -\frac{K}{2}\hat{G}(\kappa)\sin\alpha & -1 + \frac{K}{2}\hat{G}(\kappa)\cos\alpha - \lambda \end{pmatrix} = 0.$$

This yields two spectral curves

$$\lambda_{\pm}(\kappa) = -1 + \frac{K}{2}e^{\pm i\alpha}\hat{G}(\kappa)$$

parameterized by the wave number $\kappa \in \mathbb{R}$. This implies that the zero solution loses its stability for

$$\mathrm{Re}\,\lambda_{\pm}(\kappa) = \frac{K}{2}\hat{G}(\kappa)\cos\alpha - 1 = 0. \tag{9}$$

Since the coupling function is assumed to be even, unimodal, and normalized, its Fourier transform is even and has the maximum $\hat{G}(0) = 1$. Hence, (9) induces a Turing like instability with central wave number $\kappa = 0$, where for

$$K = K_T = \frac{2}{\cos\alpha}. \tag{10}$$

the zero solution becomes unstable to homogeneous perturbations and for further increasing K also for perturbations within an increasing band of wave numbers around zero.

Stability of partially coherent plane waves

In this section we present a refined linear stability analysis of the plane wave solutions

$$u(x,t) = a_0 e^{i(\kappa_0 x + \nu_0 t)}, \tag{11}$$

which bifurcate from the zero solution at the Turing like instability (9). In order to simplify the notation, we rescale the coupling parameter by

$$\tilde{K} = \frac{K}{2}\cos\alpha - 1, \tag{12}$$

such that the destabilization of the zero solution (9) occurs for $\tilde{K} = 0$, independent on α. The bifurcating wave solutions (11) have to satisfy

$$\hat{G}(\kappa_0) = \frac{1}{(1-a_0^2)(\tilde{K}+1)} \tag{13}$$

and

$$\nu_0 = -\tan\alpha\frac{1+a_0^2}{1-a_0^2}. \tag{14}$$

Note that in this way we obtain a branch of solutions satisfying the inequality $0 \leq a_0 \leq 1$ and hence remaining within the invariant set $|u| \leq 1$ of solutions of the Ott-Antonsen equation (2) that can be related to the oscillator system (1) . Recall that admissible solutions satisfy the inequality $0 \leq a_0 \leq 1$. To study the stability of such plane wave solutions, we transform Eq. (2) into corotating coordinates

$$U(x,t) = u(x,t)e^{-i(\kappa_0 x + \nu_0 t)}$$

and linearize the resulting equation at a wave solution, now represented by

$$U(x,t) = a_0$$

with a_0, κ_0, ν_0 satisfying (13) and (14). Small perturbations v follow the equation

$$\frac{dv}{dt} = -(1+i\nu_0)v + \frac{K}{2}e^{-i\alpha}\mathcal{J}_1 v - \frac{K}{2}e^{i\alpha}a_0^2(\mathcal{J}_2 v + 2\hat{G}(\kappa_0)v),$$

where we used the fact that $\hat{G}$ is an even function and abbreviated

$$(\mathcal{J}_1 v)(x) = \int_{-\infty}^{\infty} G(x-y)e^{-i\kappa_0(x-y)}v(y,t)dy,$$

$$(\mathcal{J}_2 v)(x) = \int_{-\infty}^{\infty} G(x-y)e^{i\kappa_0(x-y)}\overline{v}(y,t)dy.$$

Using (12), (13), and (14), we can rewrite this equation as

$$\frac{dv}{dt} = \frac{(1-i\tan\alpha)(\mathcal{J}_1 v - \hat{G}(\kappa_0)v) - a_0^2(1+i\tan\alpha)(\mathcal{J}_2 v + \hat{G}(\kappa_0)v)}{(1-a_0^2)\hat{G}(\kappa_0)}. \tag{15}$$

In order to deal with the complex conjugation of the unknown v in $\mathcal{J}_2$, we will rewrite this equation as a system in $\mathbb{R}^2$ for

$$V(x,t) = \begin{pmatrix} \operatorname{Re} v(x,t) \\ \operatorname{Im} v(x,t) \end{pmatrix}.$$

To this end, we insert in (15) the real expressions

$$(\mathcal{J}_1 v)(x,t) = \int_{-\infty}^{\infty} G(x-y)\begin{pmatrix} \cos\kappa_0(x-y) & \sin\kappa_0(x-y) \\ -\sin\kappa_0(x-y) & \cos\kappa_0(x-y) \end{pmatrix} V(y,t)dy, \tag{16}$$

$$(\mathcal{J}_2 v)(x,t) = \int_{-\infty}^{\infty} G(x-y)\begin{pmatrix} \cos\kappa_0(x-y) & \sin\kappa_0(x-y) \\ \sin\kappa_0(x-y) & -\cos\kappa_0(x-y) \end{pmatrix} V(y,t)dy \tag{17}$$

for the integrals and replace the complex numbers

$$1 \pm i\tan\alpha \quad \text{with corresponding real matrices} \quad \begin{pmatrix} 1 & \mp\tan\alpha \\ \pm\tan\alpha & 1 \end{pmatrix}. \tag{18}$$

Solving the resulting system for eigenfunctions of the form (7) and using the identity (8) we can evaluate the integrals

$$\mathcal{J}_1(V_0 e^{i\kappa x}) = \begin{pmatrix} h_+(\kappa,\kappa_0) & ih_-(\kappa,\kappa_0) \\ -ih_-(\kappa,\kappa_0) & h_+(\kappa,\kappa_0) \end{pmatrix} V_0 e^{i\kappa x}, \tag{19}$$

$$\mathcal{J}_2(V_0 e^{i\kappa x}) = \begin{pmatrix} h_+(\kappa,\kappa_0) & ih_-(\kappa,\kappa_0) \\ ih_-(\kappa,\kappa_0) & -h_+(\kappa,\kappa_0) \end{pmatrix} V_0 e^{i\kappa x}, \tag{20}$$

where

$$h_+(\kappa,\kappa_0) = \frac{1}{2}\left(\hat{G}(\kappa+\kappa_0)+\hat{G}(\kappa-\kappa_0)\right), \quad (21)$$

$$h_-(\kappa,\kappa_0) = \frac{1}{2}\left(\hat{G}(\kappa+\kappa_0)-\hat{G}(\kappa-\kappa_0)\right), \quad (22)$$

and, using

$$A = \frac{1+a_0^2}{1-a_0^2}.$$

we remain with the characteristic equation

$$\chi(\lambda) = \det\begin{pmatrix} -A+\dfrac{h_+ - ih_-\tan\alpha}{\hat{G}(\kappa_0)} - \lambda & -\tan\alpha + \dfrac{h_+\tan\alpha + ih_-}{\hat{G}(\kappa_0)} \\ \tan\alpha - \dfrac{A(h_+\tan\alpha + ih_-)}{\hat{G}(\kappa_0)} & -A + \dfrac{A(h_+ - ih_-\tan\alpha)}{\hat{G}(\kappa_0)} - \lambda \end{pmatrix} = 0 \quad (23)$$

for the complex eigenvalues $\lambda(\kappa)$.

For each plane wave solution (11) with amplitude a_0 and wave number κ_0 equation (23) provides two branches of eigenvalues $\lambda_{1,2}(\kappa)$, which are parameterized by the wave number of the perturbation κ. The corresponding value of the parameter $\tilde{K}$ has to be determined from (13). Inserting $\kappa = 0$ into (23) and using the fact that for even functions $\hat{G}(\kappa_0)$ we have

$$h_+(0,\kappa_0) = \hat{G}(\kappa_0), \quad (24)$$

$$h_-(0,\kappa_0) = 0, \quad (25)$$

we obtain two roots: the trivial eigenvalue $\lambda_{\rm c}(0) = 0$ enforced by the phase shift along the primary periodic wave solution, and

$$\lambda_{\rm s}(0) = -\frac{2a_0^2}{1-a_0^2},$$

providing a stable eigenvalue for homogeneous perturbations with $\kappa = 0$.

For the Benjamin-Feir type instability we are interested in the critical branch $\lambda_{\rm c}(\kappa)$, satisfying $\lambda_{\rm c}(0) = 0$, which at the onset of instability changes its curvature $\lambda_c''(0)$ from negative to positive, such that the curve protrudes into the unstable half plane with $\lambda(\kappa) > 0$ for κ close to zero, in this way giving rise to a long wave instability [2, 3]. In order to evaluate this instability condition, we want now to expand $\lambda_{\rm c}(\kappa)$ around its root at $\kappa = 0$. To this end, we perform twice an implicit differentiation with respect to κ of the quadratic polynomial equation $\chi(\lambda) = 0$ and insert $\kappa = 0$ and $\lambda(0) = \lambda_{\rm c}(0) = 0$ into the result. Moreover, using the assumption that $\hat{G}$ is an even function, we obtain from (21) and (22)

$$\left.\frac{\partial h_+(\kappa,\kappa_0)}{\partial\kappa}\right|_{\kappa=0} = 0, \qquad \left.\frac{\partial h_-(\kappa,\kappa_0)}{\partial\kappa}\right|_{\kappa=0} = \hat{G}'(\kappa_0)$$

and

$$\left.\frac{\partial^2 h_+(\kappa,\kappa_0)}{\partial\kappa^2}\right|_{\kappa=0} = \hat{G}''(\kappa_0), \qquad \left.\frac{\partial^2 h_-(\kappa,\kappa_0)}{\partial\kappa^2}\right|_{\kappa=0} = 0.$$

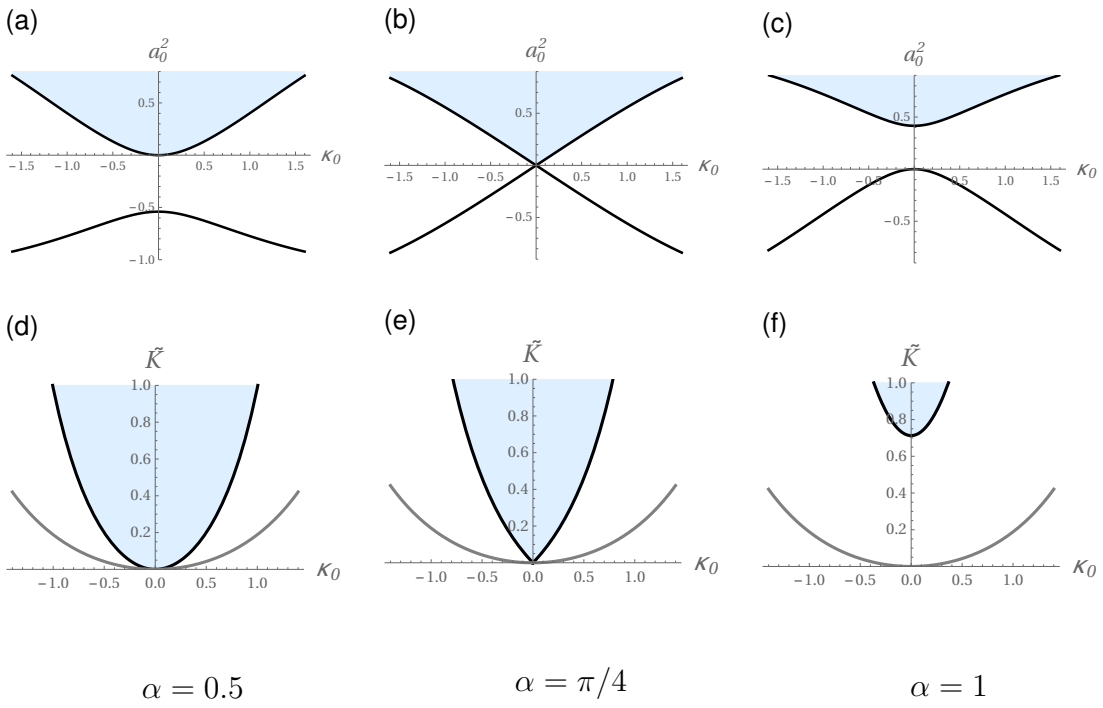

Figure 1: (Color online) Bifurcation curves and stability regions for different values of the phase lag parameter α

Using these expressions, we obtain from the first derivative that

$$\lambda_c'(0) = \frac{2i\hat{G}'(\kappa_0)\tan\alpha}{(1-a_0^2)\hat{G}(\kappa_0)}. \tag{26}$$

From the second derivative we obtain, using also (26)

$$\lambda_c''(0) = \frac{a_0^4(\hat{G}''(\kappa_0)\hat{G}(\kappa_0) - \hat{G}'(\kappa_0)^2) + a_0^2\hat{G}''(\kappa_0)\hat{G}(\kappa_0)\cos 2\alpha + \hat{G}'(\kappa_0)^2}{a_0^2\hat{G}(\kappa_0)^2(1-a_0^2)(\tan^2\alpha + 1)}, \tag{27}$$

such that the bifurcation condition $\lambda_c''(0) = 0$ is given by

$$a_0^4(\hat{G}''(\kappa_0)\hat{G}(\kappa_0) - \hat{G}'(\kappa_0)^2) + a_0^2\hat{G}''(\kappa_0)\hat{G}(\kappa_0)\cos 2\alpha + \hat{G}'(\kappa_0)^2 = 0. \tag{28}$$

Let us first discuss the stability of wave solutions with wave number $\kappa_0 = 0$, which is the central wavelength of the Turing like instability of the zero solution. Recall that $\hat{G}(0) = 1$, $\hat{G}'(0) = 0$, and $\hat{G}''(0) < 0$. Hence, we can conclude from the signs of the leading terms of (27) that for sufficiently large amplitude a_0 the stability condition $\lambda_c''(0) < 0$ is satisfied. Moreover, for $\kappa_0 = 0$ the roots of the bifurcation condition (28), which is a quadratic polynomial in a_0^2, are given by

$$a_0^2 = 0 \quad \text{and} \quad a_0^2 = -\cos 2\alpha. \tag{29}$$

For $\alpha > \frac{\pi}{4}$, the second root is positive and we can conclude that plane wave solutions with $\kappa_0 = 0$ and amplitudes satisfying

$$0 < a_0^2 < -\cos 2\alpha$$

are unstable. Figure 1 shows the roots of the bifurcation condition and the stability regions also for $\kappa_0 \neq 0$. For these plots, we had to specify coupling function and our choice is a simple piecewise constant coupling function with

$$\hat{G}(\kappa_0) = \frac{\sin \kappa_0}{\kappa_0}$$

as already used in [24]. The Figure shows three qualitatively different cases occurring for different values of the phase lag parameter α. In the upper panels (a)–(c) the branch of roots of the bifurcation condition (28) with $a_0^2(\kappa_0) \geq 0$ delimits the region of wave numbers κ_0 and amplitudes a_0 where the corresponding plane wave solution (13) is stable (shaded). There is also a second branch with $a_0^2(\kappa_0) \leq 0$, which is irrelevant as a stability boundary but will become important for the degeneracy at $\alpha = \frac{\pi}{4}$, which we discuss below. Inserting (10) into the non-negative branch, we plotted in panels (d)–(f) the stability region where for a given coupling parameter $\tilde{K}$ the plane wave solution with wave number κ_0 is stable. In addition we plotted here also the instability (9) of the zero solution, where plane wave solution with wave number κ_0 bifurcate from the trivial solution (gray line in panels (d)–(f)). This corresponds to $a_0 = 0$ in the upper panels.

For $\alpha < \pi/4$ we observe the well known Eckhaus scenario [9], see panels (a),(d). Here, at $\tilde{K} = 0$ the zero solutions becomes unstable with respect to perturbations with the central wave number $\kappa_0 = 0$ and a stable branch of non-trivial solutions bifurcates. Increasing $\tilde{K}$ further, subsequently also perturbations of the zero solutions with non-zero wave number start to grow. But the corresponding plane wave solutions bifurcate unstable from the already unstable zero solution and gain their stability only at some larger amplitude $a_0 > 0$, given by the bifurcation condition (28).

For $\alpha > \pi/4$ the situation is qualitatively different, see panels (c),(f) in Fig. 1. All plane wave solutions bifurcate unstable from the zero solution and gain their stability only at a positive amplitude a_0.

A codimension-two bifurcation

For $\alpha = \frac{\pi}{4}$ there is a singularity, where zero is a double root of the bifurcation condition, see panel (b) in Fig. 1. This is due to the fact that in (28) the coefficient $\cos 2\alpha$ of the a_0^2 term changes its sign. This codimension two bifurcation at $\alpha = \frac{\pi}{4}$, $\tilde{K} = 0$ mediates the transition between the two different types of codimension one bifurcations described above. Note that by symmetry reasons, the onset of Benjamin-Feir stability happens also for $\alpha > \frac{\pi}{4}$ always at the central wave number $\kappa_0 = 0$. Hence, the boundary of the parameter region where Benjamin-Feir stable waves exist can be expressed in the parameters α and $\tilde{K}$ by using the roots (29) and (13) to eliminate the amplitude a_0. In this way we obtain

$$\tilde{K} = \begin{cases} 0 & \text{for} \quad \alpha < \frac{\pi}{4}, \\ \frac{\tan^2 \alpha - 1}{2} & \text{for} \quad \alpha \geq \frac{\pi}{4}. \end{cases} \tag{30}$$

Note that at $\alpha = \frac{\pi}{4}$ we have to switch between the two branches (29) of roots of the bifurcation condition. For the original coupling strength K we obtain from (12) for the boundary of the

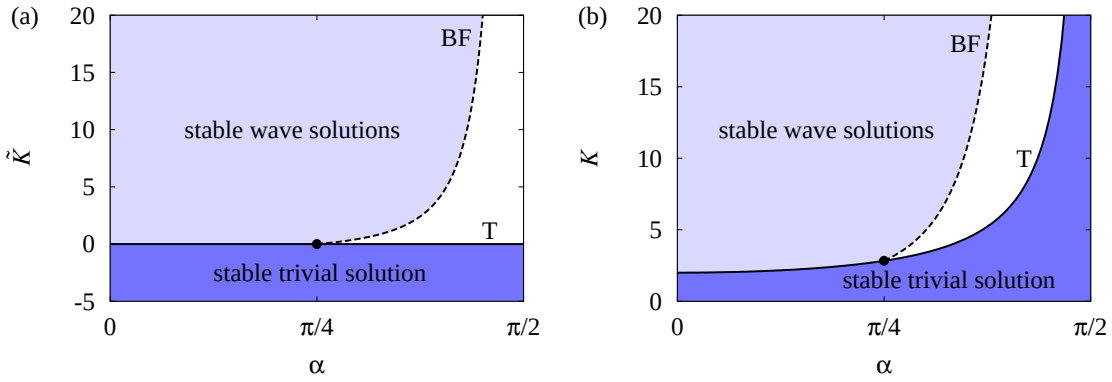

Figure 2: (Color online) Parameter regions where the trivial solution is stable (dark shaded), Benjamin-Feir stable waves exist (light shaded), irregular dynamics (white), separated by the instability of the zero solution (solid line) and Benjamin-Feir condition (dashed line); left panel: rescaled coupling strength $\tilde{K}$ versus α, right panel: original coupling strength K versus α.

parameter region where Benjamin-Feir stable waves exist the condition

$$K = \begin{cases} \frac{2}{\cos\alpha} & \text{for} \quad \alpha < \frac{\pi}{4}, \\ \frac{1}{\cos^3\alpha} & \text{for} \quad \alpha \geq \frac{\pi}{4}. \end{cases} \tag{31}$$

In Fig. 2 we have plotted the Benjamin-Feir stable regions according to the stability boundary (30) for the parameter $\tilde{K}$ versus α (left panel) and (31) for the original parameter K versus α (right panel) together with the corresponding stability region for the trivial solution, given by the instability (9). One can see that at the codimension two point $\alpha = \frac{\pi}{4}$, $\tilde{K} = 0$ there emerges a Benjamin-Feir unstable window at small amplitudes.

Phase turbulence and amplitude turbulence

Figure 2 shows that there is a parameter region where the trivial solution $u(x,t) = 0$ and all wave solutions (11) turn out to be unstable simultaneously. In order to investigate the dynamics for such parameters (α, K) we performed a numerical study of Eq. (2). For this purpose, we introduced periodic boundary conditions on the interval $x \in [0, 50]$, choosing the interval length sufficiently large with respect to the coupling radius, such that boundary effects play no important role here. We used a space discretization on a uniform grid with $N = 2000$ points and performed a time integration of the resulting discretized version of Eq. (2) using the fourth-order Runge-Kutta scheme with a time step $dt = 0.02$. As initial data we took randomly generated sequences of complex numbers satisfying the inequality $|u| < 1$.

Similar as in the classical results for the complex cubic Ginzburg-Landau equation in the Benjamin-Feir unstable regime [30, 6, 4, 5], we observe two qualitatively different types of spatio-temporal chaos, which are called phase turbulence and amplitude (or defect) turbulence. Phase turbulence is characterized by the fact that the absolute value $|u(x,t)|$ remains uniformly bounded from zero and irregular fluctuations occur mainly in the complex phase, see Figure 3 (a),(b).

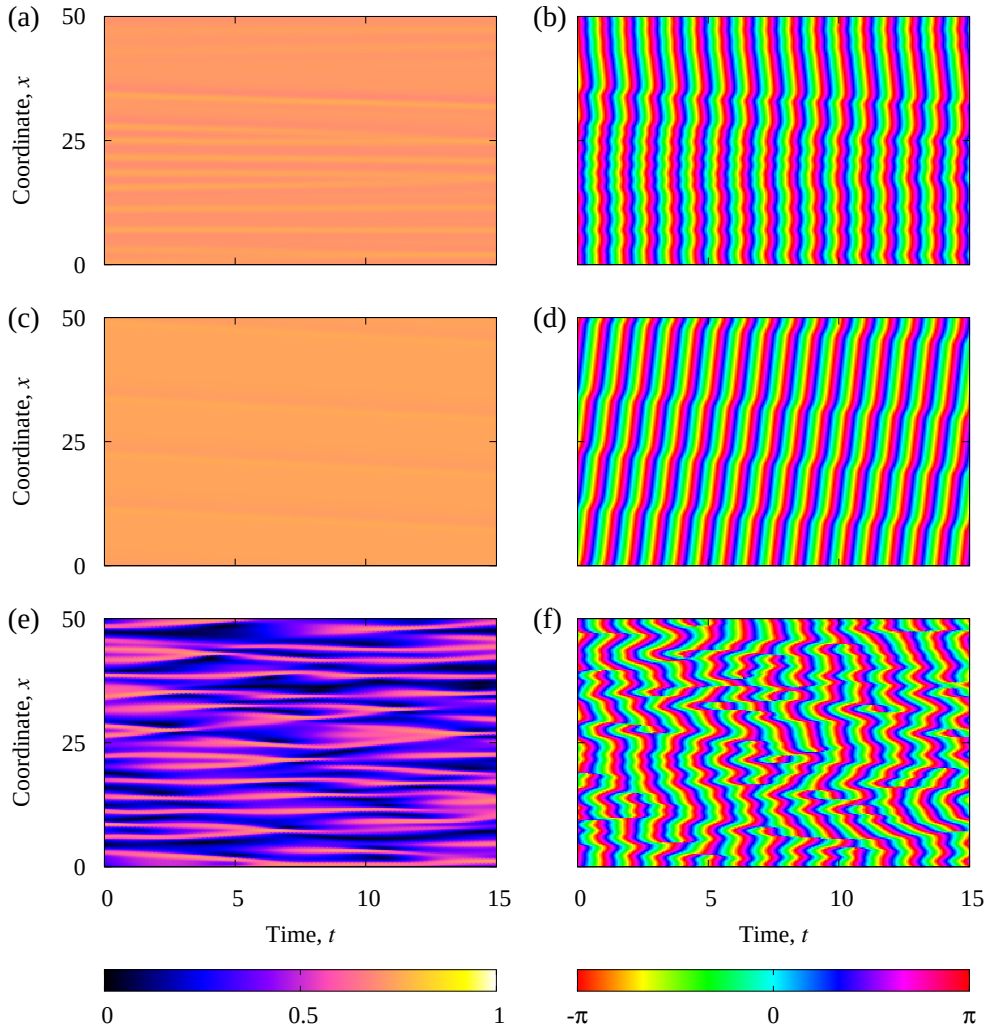

Figure 3: (Color online) Space-time plots of $|u(x,t)|$ and $\arg u(x,t)$ of turbulent solutions for Eq. (2) with periodic boundary conditions on the interval $x \in [0, 50]$. (a), (b) Phase turbulence ($\alpha = 1.14$), (c), (d) Twisted phase turbulence ($\alpha = 1.11$), (e), (f) Amplitude turbulence ($\alpha = 1.25$). Other parameters: $K = 10$.

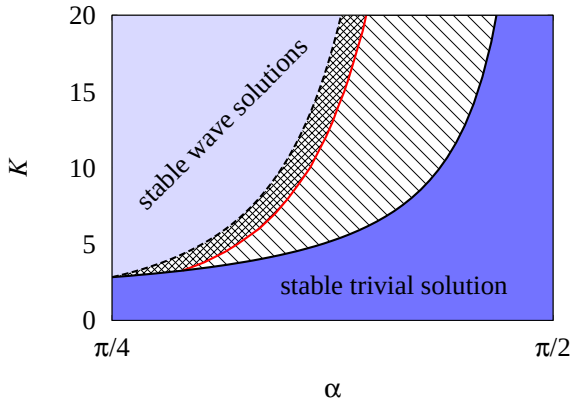

Figure 4: (Color online) The region between Benjamin-Feir instability of planar wave solutions (dashed line) and instability of the trivial solution (solid line) is divided into regions of phase turbulence (shaded) and amplitude turbulence (hatched).

For the amplitude turbulence, the absolute value $|u(x,t)|$ vanishes at some locations in space and time developing phase singularities, called 'defects', see Figure 3 (e),(f). Note that starting from a stable wave with $\kappa \neq 0$ and decreasing the parameter K or α below one can also obtain twisted phase turbulence, i.e. a irregular wave solution with a fixed non-zero average wave number, see Fig. 3 (c),(d).

For a numerical detection of the two distinct dynamical regimes of phase and amplitude turbulence, we employed the following procedure in our simulations: After discarding a transient of 10000 time units we recorded the global minimum and maximum of $|u(x,t)|$ within another time interval of the length 10000. While for the trivial solution $|u(x,t)| = 0$ and for a wave solution (11) we have $|u(x,t)| = a_0$, and hence the minimum and maximum coincide, for phase and amplitude turbulence these two quantities differ from each other. It turns out that there is a clear distinction between the phase turbulence regime, where the minimum is strictly positive and the amplitude turbulence where the minimum is zero.

Scanning in this way the Benjamin-Feir unstable parameter region, we obtained the bifurcation diagram given in Fig. 4 where the red curve indicates the transition from phase turbulence to amplitude turbulence. In our simulations, we did not find any indications for a extended region of bistability between the two irregular regimes or a region of spatio-temporal intermittency, where amplitude turbulence coexists with stable plane waves, as it is reported for certain parameter regions in the Ginzburg-Landau equation [6]. Indeed, performing the parameter scans as a dynamical continuation, where the final state of each simulation is used as an initial condition for the next parameter value, we found that forward and backward scans provide only a very slight deviation (below the resolution of the diagram) in the location of the transition.

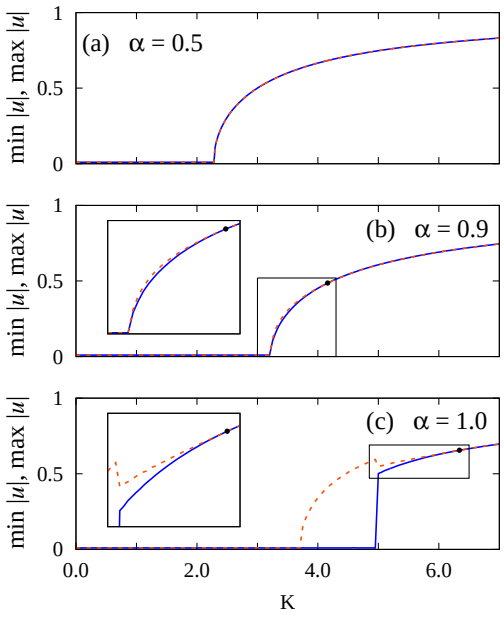

Figure 5: (Color online) Synchronization transitions from complete incoherence to partial coherence for different values of the phase lag parameter α. (a) direct transition; (b) transition with intermediate stage of partially coherent phase turbulence; (c) transition with intermediate stages of partially coherent amplitude and phase turbulence;

Synchronization transitions

Following the classical paradigm of Kuramoto, increasing the coupling strength K in a globally coupled population of heterogeneous oscillators there is a threshold value where a transition from complete incoherence to partial synchrony can be observed. The phase lag parameter α plays here no crucial role. Staying in the attracting regime $\alpha < \pi/2$, the synchronization transition remains qualitatively unchanged and only the critical coupling strength increases with increasing α. As it has been shown in [24] in spatially extended systems, after the destabilization of the completely incoherent state there appear also partially coherent plane wave solutions. However, they emerge unstable and for increasing coupling strength, one will observe a transition from the completely incoherent state to a spatially homogeneous partial synchrony, see Fig. 5(a) showing the transition for $\alpha = 0.5$.

In spatially extended systems the situation is fundamentally different for $\alpha > \pi/4$. In this case the system enters above the synchronization threshold into a state where locally in x the oscillators are in partial synchrony. However, the Ott-Antonsen system (2) is in the Benjamin-Feir unstable regime and we observe irregular macroscopic fluctuations of the local order parameter $u(x,t)$. Depending on the value of α, the system can either immediately enter in a state of macroscopic phase turbulence before for further increased coupling it reaches the region of stable spatially homogeneous partial synchrony, see Fig. 5(b), or first enter into the region of amplitude turbulence before passing through the region of phase turbulence into the Benjamin-Feir stable regime, see Fig. 5(c). In Fig. 5 we display the maximum (dashed, red) and minimum (solid, blue) of $|u(x,t)|$. Note that these two values coincide for complete incoherence and spa-

tially homogeneous partial synchrony, while they slightly differ in the region of phase turbulence (panels b,c). Finally, in the region of amplitude turbulence the minimum stays at zero, while the maximum shows the growing amplitude of the turbulent state.

References

[1] D. M. Abrams and S. H. Strogatz, "Chimera states for coupled oscillators", Phys. Rev. Lett. **93**, p. 174102 (2004).

[2] T. B. Benjamin, "Instability of periodic wavetrains in nonlinear dispersive systems", Proc. Roy. Soc. A **299**, pp. 59–75 (1967).

[3] T. B. Benjamin and J. E. Feir, "The disintegration of wave trains on deep water. Part 1. Theory", J. Fluid Mech. **27**, pp. 417–430 (1967).

[4] L. Brusch, M. G. Zimmermann, M. van Hecke, M. Bär, and A. Torcini, "Modulated amplitude waves and the transition from phase to defect chaos", Phys. Rev. Lett. **85**, p. 86 (2000).

[5] L. Brusch, A. Torcini, M. van Hecke, M. G. Zimmermann, and M. Bär, "Modulated amplitude waves and defect formation in the one-dimensional complex Ginzburg-Landau equation", Physica D **160**, pp. 127–148 (2001).

[6] H. Chaté, "Spatio-temporal intermittency regimes of the one-dimensional complex Ginzburg-Landau equation", Nonlinearity **7**, pp. 185–204 (1994).

[7] H. Chiba and I. Nishikawa, "Center manifold reduction for large populations of globally coupled phase oscillators", Chaos **21**, p. 043103 (2011).

[8] J. D. Crawford and K. T. R. Davies, "Synchronization of globally coupled phase oscillators: Singularities and scaling for general couplings", Physica D **125**, pp. 1–46 (1999).

[9] W. Eckhaus, "Studies in Nonlinear Stability Theory", Springer, Berlin, 1965.

[10] A. M. Hagerstrom, T. E. Murphy, R. Roy, P. Hövel, I. Omelchenko, and E. Shöll, "Experimental observation of chimeras in coupled-map lattices", Nature Phys. **8**, pp. 658–661 (2012).

[11] T. Kapitaniak, P. Kuzma, J. Wojewoda, K. Czolczynski, and Y. Maistrenko, "Imperfect chimera states for coupled pendula", Sci. Rep. **4**, p. 6379 (2014).

[12] M. Komarov and A. Pikovsky, "Multiplicity of singular synchronous states in the Kuramoto model of coupled oscillators", Phys. Rev. Lett. **111**, p. 204101 (2013).

[13] Y. Kuramoto, in: H. Arakai (Ed.), International Symposium on Mathematical Problems in Theoretical Physics, Lecture Notes in Physics, Vol 39, Springer, New York, 1975, p. 420.

[14] Y. Kuramoto and D. Battogtokh, "Coexistence of coherence and incoherence in nonlocally coupled phase oscillators", Nonlinear Phenom. Complex Syst. **5**, pp. 380–385 (2002).

[15] C. Laing, “The dynamics of chimera states in heterogeneous Kuramoto networks”, Physica D **238**, pp. 1569–1588 (2009).

[16] C. R. Laing, “Derivation of a neural field model from a network of theta neurons”, Phys. Rev. E **90**, p. 010901 (2014).

[17] W. S. Lee, J. G. Restrepo, E. Ott, and T. M. Antonsen, “Dynamics and pattern formation in large systems of spatially-coupled oscillators with finite response times”, Chaos **21**, p. 023122 (2011).

[18] T. B. Luke, E. Barreto, and P. So, “Complete classification of the macroscopic behavior of a heterogeneous network of theta neurons”, Neural Computation **25** (2013), pp. 3207–3234.

[19] E. A. Martens, E. Barreto, S. H. Strogatz, E. Ott, P. So, and T. M. Antonsen, “Exact results for the Kuramoto model with a bimodal frequency distribution”, Phys. Rev. E **79**, p. 026204 (2009).

[20] E. A. Martens, S. Thutupalli, A. Fourrire, and O. Hallatschek, “Chimera states in mechanical oscillator networks”, Proc. Natl Acad. Sci. USA **110**, p. 10563–10567 (2013).

[21] O. Omel’chenko, “Coherence-incoherence patterns in a ring of non-locally coupled phase oscillators”, Nonlinearity **26**, pp. 2469–2498 (2013).

[22] O. Omel’chenko and M. Wolfrum, “Nonuniversal transitions to synchrony in the Sakaguchi-Kuramoto model”, Phys. Rev. Lett. **109**, p. 164101 (2012).

[23] O. Omel’chenko and M. Wolfrum, “Bifurcations in the Sakaguchi-Kuramoto model”, Physica D **263**, p. 74–85 (2013).

[24] O. Omel’chenko, M. Wolfrum, and C. Laing, “Partially coherent twisted states in arrays of coupled phase oscillators”, Chaos **24**, p. 023102 (2014).

[25] E. Ott and T. M. Antonsen, “Low dimensional behavior of large systems of globally coupled oscillators”, Chaos **18**, p. 037113 (2008).

[26] E. Ott and T. M. Antonsen, “Long time evolution of phase oscillator systems ”, Chaos **19**, p. 023117 (2009).

[27] M. J. Panaggio and D. M. Abrams, “Chimera states: coexistence of coherence and incoherence in networks of coupled oscillators”, Nonlinearity **28**, pp. R67–R87 (2015).

[28] D. Pazó and E. Montbrió, “Low-dimensional dynamics of populations of pulse-coupled oscillators”, Phys. Rev. X **4**, p. 011009 (2014).

[29] L. Schmidt, K. Schönleber, K. Krischer, and V. Garcia-Morales, “Coexistence of synchrony and incoherence in oscillatory media under nonlinear global coupling”, Chaos **24**, p. 013102 (2014).

[30] B. I. Shraiman, A. Pumir, W. van Saarloos, P. C. Hohenberg, H. Chaté, and M. Holen, “Spatiotemporal chaos in the one-dimensional complex Ginzburg-Landau equation”, Physica D **57**, pp. 241–248 (1992).

[31] S.H. Strogatz, “ From Kuramoto to Crawford: Exploring the onset of synchronization in populations of coupled oscillators”, Physica D **143**, pp. 1–20 (2000).

[32] M. R. Tinsley, S. Nkomo, and K. Showalter, “Chimera and phase-cluster states in populations of coupled chemical oscillators”, Nature Phys. **8**, pp. 662–665 (2012).

[33] D. Wiley, S. Strogatz, and M. Girvan, "The size of the sync basin", Chaos **16**, p. 015103 (2006).